European Journal of Pharmacology 894 (2021) 173853

Contents lists available at ScienceDirect

European Journal of Pharmacology

journal homepage: www.elsevier.com/locate/ejphar

Synthetic cyclopenta[*b*]indoles exhibit antineoplastic activity by targeting microtubule dynamics in acute myeloid leukemia cells

Hugo Passos Vicari [a], Keli Lima [a], Ralph da Costa Gomes [b], Daniara Cristina Fernandes [b,c], Jean Carlos Lipreri da Silva [a], Manoel Trindade Rodrigues Junior [b], Aline Silva Barroso de Oliveira [b], Ricardo Nascimento dos Santos [d], Adriano Defini Andricopulo [d], Fernando Coelho [b], Leticia Veras Costa-Lotufo [a], João Agostinho Machado-Neto [a,*]

[a] *Department of Pharmacology, Institute of Biomedical Sciences, University of São Paulo, São Paulo, SP, 05508-900, Brazil*
[b] *Department of Organic Chemistry, Chemistry Institute, University of Campinas, Campinas, São Paulo, SP, 13083-970, Brazil*
[c] *Currently at Instituto Federal de Educação Ciência e Tecnologia de São Paulo, Matão, SP, 15991-502, Brazil*
[d] *Physics Institute of São Carlos, University of São Paulo, São Carlos, SP, 13565-905, Brazil*

ARTICLE INFO

Keywords:
cyclopenta[*b*]indoles
Acute promyelocytic leukemia
Microtubule dynamics
Chemotherapy resistance

ABSTRACT

Acute promyelocytic leukemia (APL) is associated with PML-RARα oncogene, which is treated using all-*trans* retinoic acid (ATRA)-based chemotherapy. However, chemoresistance is observed in 20–30% of treated patients and represents a clinical challenge, raising the importance of the development of new therapeutic options. In the present study, the effects of three synthetic cyclopenta[*b*]indoles on the leukemia phenotype were investigated using NB4 (ATRA-sensitive) and NB4-R2 (ATRA-resistant) cells. Among the tested synthetic cyclopenta[*b*]indoles, compound **2**, which contains a heterocyclic nucleus, was the most active, presenting time-dependent cytotoxic activity in the μM range in APL cells, without cytotoxicity for normal leukocytes, and was selected for further characterization. Compound **2** significantly decreased clonogenicity, increased apoptosis, and caused cell cycle arrest at S and G_2/M phases in a drug concentration-dependent manner. Morphological analyses indicated aberrant mitosis and diffuse tubulin staining upon compound **2** exposure, which corroborates cell cycle findings. In the molecular scenario, compound **2** reduced STMN1 expression and activity, and induced PARP1 cleavage and H2AX and CHK2 phosphorylation, and modulated *CDKN1A*, *PMAIP1*, *GADD45A*, and *XRCC3* expressions, indicating reduction of cell proliferation, apoptosis, and DNA damage. Moreover, in the *in vivo* tubulin polymerization assay, NB4 and NB4-R2 cells showed a reduction in the levels of polymerized tubulin upon compound **2** exposure, which indicates tubulin as a target of the drug. Molecular *docking* supports this hypothesis. Taken together, these data indicated that compound **2** exhibits antileukemic effects through disrupting the microtubule dynamics, identifying a possible novel potential antineoplastic agent for the treatment of ATRA-resistant APL.

1. Introduction

Acute myeloid leukemia (AML) is a heterogeneous hematopoietic system-related cancer characterized by abnormal clonal proliferation and impaired differentiation of myeloid precursors (De Kouchkovsky and Abdul-Hay, 2016; Short et al., 2018). Acute promyelocytic leukemia (APL) is AML subtype characterized by bone marrow infiltration by promyelocyte-like blasts, which corresponds to the M3 and M3 variant subtypes (M3v) according to the French-American-British classification, and AML subtype associated with a translocation between chromosomes 15 and 17 [t (15; 17)] and variants according to the World Health Organization classification (Arber et al., 2016; Bennett et al., 1976; Van den Berghe, 1988). Indeed, approximately 90% of APL cases are associated with t(15; 17) (q22; q21) translocation, resulting in the fusion of the PML (promyelocytic leukemia) and RARα (alpha retinoic acid receptor) genes and creating the hybrid oncogene PML-RARα (Melnick

* Corresponding author. Department of Pharmacology Institute of Biomedical Sciences of University of São Paulo Av. Prof. Lineu Prestes, 1524CEP 05508-900, São Paulo, SP, Brazil.
E-mail address: jamachadoneto@usp.br (J.A. Machado-Neto).

https://doi.org/10.1016/j.ejphar.2021.173853
Received 26 August 2020; Received in revised form 11 December 2020; Accepted 5 January 2021
Available online 8 January 2021

and Licht, 1999; Rowley et al., 1977), which has successfully been targeted by all-trans retinoic acid (ATRA) and/or arsenic trioxide (ATO) (Avvisati et al., 2001; Reiter et al., 2004; Sanz et al., 2009; Wang and Chen, 2008).

The main mechanisms related to ATRA resistance in APL patients are genetic mutations in the RARα domain, fusions of the RARα gene with other genes limiting the therapeutic effectiveness of ATRA, increased ATRA catabolism, presence of the acid-binding protein cytoplasmic retinoic (CRABP), and the abnormal passage from ATRA to the cell nucleus (Duprez et al., 1992; Kitamura et al., 1997; Nason-Burchenal et al., 1997). Although the good clinical response of most ATRA-treated APL patients, relapse still occurs in about 20–30% of these patients and clinical resistance to ATRA represents a therapeutic challenge.

Therefore, the discovery and development of new therapeutic molecules become of great importance in the field. Cyclopenta[*b*]indoles are present in several biologically active natural and synthetic compounds, being directly responsible for their biological effects (Qiao et al., 2010; Ratni et al., 2009; Roll et al., 2009; Talaz et al., 2009). Recently, our research group synthesized new molecules with the structure based on cyclopenta[*b*]indole, and the analysis of the cytotoxic activity of these compounds in solid tumors showed the ability to disrupting tubulin microtubules and to inhibit cell migration (Santos et al., 2016). In the present study, we characterized the antileukemia activity of a novel series of three synthetic enantiomerically pure cyclopenta[*b*]indoles in ATRA-sensitive and -resistant APL cellular models.

2. Material and methods

2.1. Cell culture and reagent chemicals

Acute myeloid leukemia cell lines sensitive to ATRA (NB4) and resistant to ATRA (NB4-R2) were kindly provided by Prof. Dr. Eduardo Magalhães Rego (University of São Paulo, Ribeirão Preto, Brazil). Cell lines were cultured in RPMI supplemented with 10% fetal bovine serum (FBS) and 1% penicillin/streptomycin and maintained at 5% CO_2 and 37 °C. The authenticity of the cells was determined by Short Tandem Repeat (STR). The compounds **1**, **2**, and **3** were obtained as described in Supplementary Information and prepared as a 10 mM stock solution in dimethyl sulfoxide (Me_2SO_4; DMSO). Of note, all compounds are enantiomers that present >95% of purity and absolute stereochemistry (R,

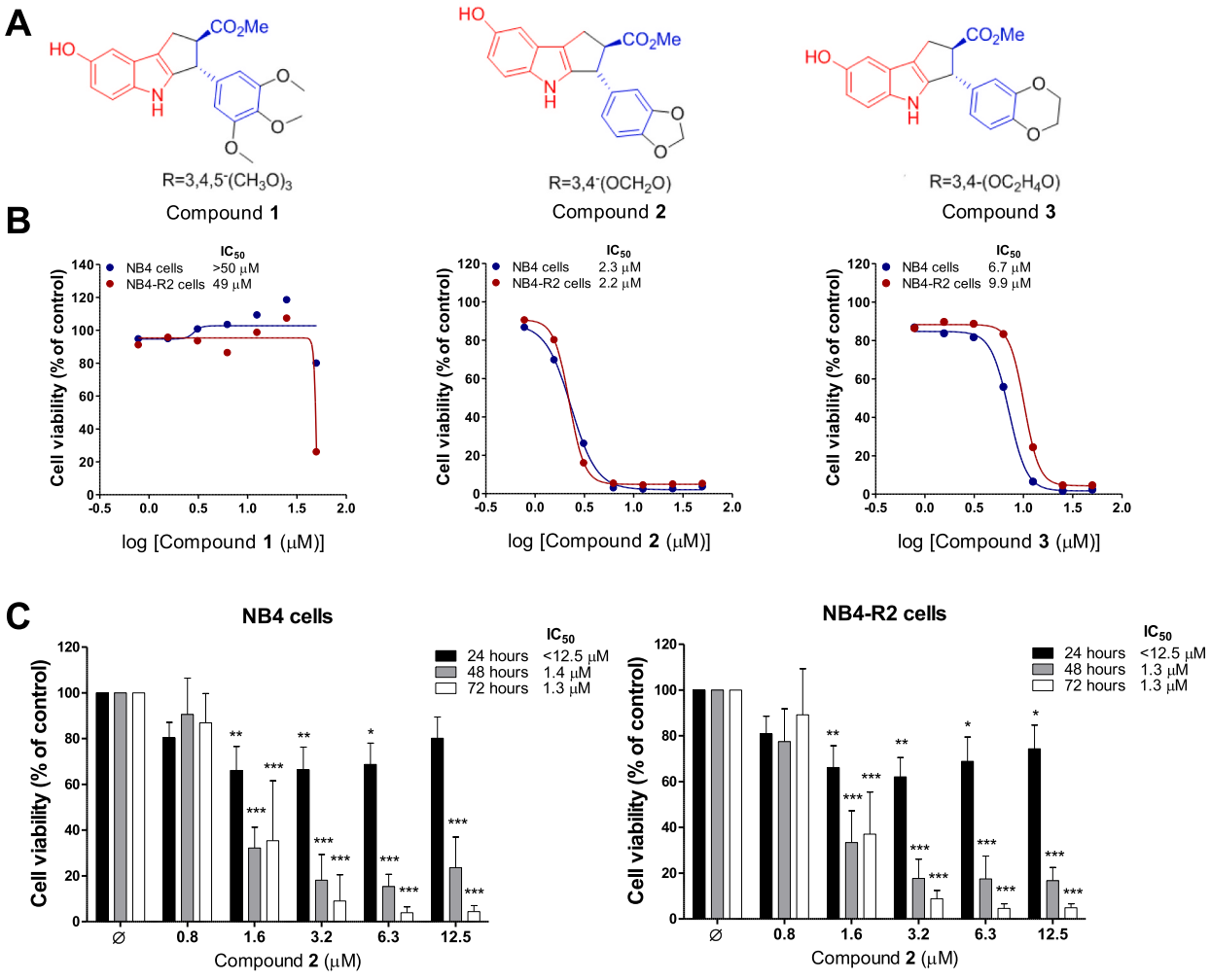

Fig. 1. Characterization of the cytotoxic activity of synthetic cyclopenta[*b*]indoles in acute myeloid leukemia cell lines. **(A)** The synthetic cyclopenta[*b*]indoles were arbitrarily named as compound **1** (molecular weight: 397.43), **2** (molecular weight: 351.36), and **3** (molecular weight: 365.39), and their molecular chemical structures are illustrated. **(B)** Dose-response curves for compound **1**, **2**, and **3** (0.8–50 μM) after 72 h of exposure in NB4 and NB4-R2 cells. The IC_{50} values of each compound are shown. **(C)** Bar graph represents to dose- and time-responses for compound **2** (0.8–12.5 μM) after 24, 48, and 72 h of exposure in NB4 and NB4-R2 cells. Values were expressed as a percentage of DMSO-treated (Ø) cells. The results are presented as mean ± S.D. of at least three independent experiments. The *P* values and cell lines are shown in the graphs: $^{*}P < 0.05$; $^{**}P < 0.01$; $^{***}P < 0.001$ for cells treated with compound **2** compared to DMSO-treated (Ø) cells; ANOVA and Bonferroni post-test.

R) for the two chiral centers. Molecular structures of the cyclopenta[*b*] indoles used are illustrated in Fig. 1A. Colchicine was obtained from Sigma-Aldrich (Sigma-Aldrich, St. Louis, MO, USA) and prepared as a 10 mM stock solution in DMSO.

2.2. Cell viability assay

To evaluate the effects on cell viability of synthesized compounds, methylthiazoletetrazolium (MTT) assays were performed. Briefly, a total of 2×10^4 cells per well were seeded in a 96-well plate and exposed to increasing concentrations of the compounds (Ø, 0.8, 1.6, 3.2, 6.3, 12.5, 25 and 50 μM) in RPMI 10% FBS for 24, 48 and/or 72 h. To evaluated cytotoxicity in normal leukocytes, peripheral blood mononuclear cells (PBMC) were obtained by Ficoll–Hypaque gradient centrifugation (Sigma-Aldrich, St Louis, MO, USA) from three healthy donors (3 males, aged 26–33 years). Informed consent was obtained from all healthy donors and the Ethics Committee of the Institute of Biomedical Sciences of the University of São Paulo approved this study (Protocol number: 4423074; CAAE: 39510920.1.0000.5467). Primary PBMC were cultured in RPMI-1640 medium containing 30% FBS, penicillin/streptomycin and recombinant cytokines (PeproTech, USA) (30 ng/ml IL3, 100 ng/ml IL7, 100 ng/ml FLT3-ligand, and 30 ng/ml SCF), at a density of 2×10^6 cells/ml, in presence of vehicle or compound **2** (Ø, 0.8, 1.6, 3.2, 6.3, 12.5, 25 and 50 μM) for 72 h. Then, after incubation, 10 μl MTT solution (5 mg/ml) was added and incubated at 37 °C, 5% CO_2 for 4 h. The reaction was stopped by using 100 μl of 0.1N HCl in anhydrous isopropanol. Cell viability was evaluated by spectrophotometry measuring the absorbance at 570 nm. The inhibitory concentration of 50% (IC_{50}) values was calculated using non-linear regression analysis on GraphPad Prism 5 (GraphPad Software, Inc., San Diego, CA, USA).

2.3. Colony formation assay

Colony formation was carried out in semisolid methylcellulose medium (0.5×10^3 cells/ml; MethoCult 4230; StemCell Technologies Inc., Vancouver, BC, Canada) in the presence, or not, of compound **2** (0.8, 1.6 and 3.2 μM) for 8 days (long-term exposure). Colonies were detected after 8 days of culture by adding 150 μl (5 mg/ml) of MTT reagent and scored by Image J quantification software (U.S. National Institutes of Health, Bethesda, MD, USA).

2.4. Cell cycle analysis

A total of 6×10^5 cells per well were seeded in six-well plates in the presence, or not, of compound **2** (0.8, 1.6 and 3.2 μM), harvested at 48 h, fixed with 70% ethanol and stored at 4 °C for at least 2 h before analysis. Alternatively, NB4 and NB4-R2 cells were synchronized by the double thymidine block method. In brief, cells were incubated in 10% FBS RPMI plus 2 mM thymidine for 16 h (first block). Thymidine was removed by washing with PBS and fresh 10% FBS RMPI was add to release cells for 8 h. Then, cells were incubated in 10% FBS RPMI plus 2 mM thymidine for additional 16 h (second block). To release cells for cell cycle progression, thymidine was removed by washing with PBS and fresh 10% FBS RMPI with vehicle or compound **2** (3.2 μM) was add. Cells were harvested and fixed with 70% ethanol at indicated time points. Fixed cells were stained with 20 μg/ml propidium iodide (PI) containing 10 μg/ml RNase A for 30 min at room temperature in a light-protected area. DNA content distribution was acquired in a FACSCalibur cytometer (Becton-Dickinson) and analyzed using FlowJo software (Treestar, Inc.).

2.5. Apoptosis assessment by annexin V and 7AAD staining

A total of 1×10^5 cells per well were seeded in a 24-well plate in RPMI 10% FBS in the presence, or not, of compound **2** (0.8, 1.6 and 3.2 μM) for 48 h. Then, cells were washed twice with ice-cold PBS and resuspended in binding buffer containing 1 μg/ml 7AAD and 1 μg/ml annexin V-FITC. All specimens were analyzed by flow cytometry (FACSCalibur; Becton Dickinson) after incubation for 15 min at room temperature in a light-protected area. Ten thousand events were acquired for each sample, using FlowJo software (Treestar, Inc., San Carlos, CA, USA).

2.6. Western blot analysis

NB4 and NB4-R2 were treated with compound **2** (0.8, 1.6 or 3.2 μM) or vehicle for 48 h and submitted for total protein extraction using a buffer containing 100 mM Tris (pH 7.6), 1% Triton X-100, 150 mM NaCl, 2 mM PMSF, 10 mM Na_3VO_4, 100 mM NaF, 10 mM $Na_4P_2O_7$, and 4 mM EDTA. Equal amounts of protein (30 μg) of the samples were then subjected to electrophoresis on SDS-PAGE polyacrylamide gel in an electrophoresis device, followed by electrotransfer of the gel proteins to the nitrocellulose membrane. The membrane was blocked with 5% milk and then incubated with specific primary antibodies diluted in blocking buffer and then with secondary antibodies conjugated to HRP (horseradish peroxidase). Western blot analysis with the indicated antibodies was performed using the SuperSignal™ West Dura Extended Duration Substrate system (Thermo Fisher Scientific, San Jose, CA, USA) and G:BOX Chemi XX6 gel document system (Syngene, Cambridge, UK United). The antibodies against Stathmin 1 (OP18; sc-55531), p-Stathmin 1^{S16} (p-OP18 Ser16; sc-12948-R), and γH2AX (sc-517348) were obtained from Santa Cruz Biotechnology (Santa Cruz, CA, USA). The antibodies against PARP1 (#9542), GAPDH (#5174), p-$CHK2^{T68}$ (#2197), CHK2 (#6334) and α-tubulin (#2144) were from Cell Signaling Technology (Danvers, MA, USA).

2.7. Quantitative RT-PCR (qRT-PCR)

NB4 and NB4-R2 were treated with compound **2** (3.2 μM) or vehicle for 48 h and total RNA was obtained using TRIzol reagent (Thermo Fisher Scientific). cDNA was synthesized from 1 μg of RNA using a High-Capacity cDNA Reverse Transcription Kit (Thermo Fisher Scientific). Quantitative PCR (qPCR) was performed using a QuantStudio 3 Real-Time PCR System in conjunction with a SybrGreen System for the expression of DNA damage-related genes (Supplementary Table 1). *HPRT1* and *ACTB* were used as reference genes. Relative quantification values were calculated using the $2^{-\Delta\Delta CT}$ equation (Livak and Schmittgen, 2001). A negative 'No Template Control' was included for each primer pair. Data were illustrated using multiple experiment viewer (MeV) 4.9.0 software (http://www.tm4.org/mev/).

2.8. Cell morphology analysis

An amount of 1×10^5 cells was seeded per well in 24-well plates, with vehicle or compound **2** (1.6 μM) for 48 h. After the incubation, the treated cells were adhered to microscopic slides using cytospin (Serocito, Model 2400, FANEM, Brazil), and subsequent hematoxylin and eosin staining (rapid panotic). The morphological analyzes of the nucleus and cytoplasm of the treated cells were made from the visualization of them in a Leica DM 2500 optical microscope and acquisition of the photos performed by the LAS V4.6 software (Leica, Germany).

2.9. Immunofluorescence microscopy

Thymidine-synchronized NB4 and NB4-R2 cells, treated with vehicle or compound **2** were attached on coverslips coated with poly-L-lysine (1 mg/ml) 6 h after thymidine release, fixed with 3.7% formaldehyde, permeabilized with 0.5% Triton X-PBS and blocked with 3% bovine serum albumin (BSA) PBS. Cells were then incubated with anti-α-tubulin Alexa Fluor® 488 conjugate (1:200 in 3% BSA PBS, Thermo Fisher Scientific) for 12 h, and followed by PBS wash. The slides were mounted in ProLong Gold Anti-Fade Mounting Medium with DAPI (Thermo Fisher Scientific). Images were generated using fluorescence microscopy

(LionHeart FX, BioTek, Winooski, VT, USA).

2.10. Microtubule polymerization in vivo analysis

The intracellular levels of microtubule polymerization were evaluated as previously described (Mistry and Atweh, 2001) with minor modifications. Briefly, an equal number of NB4 and NB4-R2 cells (1×10^6) treated with vehicle, compound **2** (1.6 μM) or paclitaxel (5 nM) for 48 h were lysed in microtubule-stabilizing lysis buffer containing 0.1 M PIPES pH 6.9, 2 M glycerol, 5 mM MgCl2, 2 mM EGTA, 0.5% Triton X-100, 4 μM Taxol, and 5 μg/ml leupeptin and submitted to centrifugation at 20,000×g for 45 min at 22 °C. Supernatants containing soluble tubulin (soluble (S) fraction) were separated from the pellets containing the polymerized tubulin (polymerized (P) fraction). Then, pellets were solubilized in the microtubule-stabilizing buffer and subjected to ultrasonic waves for 20 min. S and P fractions were submitted to Western blot analysis for α-tubulin detection. GAPDH expression, which is presented only in S fraction, was used as control of fractionation.

2.11. Molecular modeling

For docking analysis the GOLD 5.1 software (Cambridge Crystallographic Data Centre, Cambridge, UK), crystallographic model of tubulin/colchicine (PDB 1SA0) and the structure of compounds **1**, **2** and **3** were used.

2.12. Statistical analysis

Statistical analysis was performed using GraphPad Instat 5 (GraphPad Software, Inc., San. Diego, CA, USA). For comparisons, ANOVA and Bonferroni post-test or Student *t* test were used. A *P*-value < 0.05 was considered as statistically significant.

3. Results

3.1. Cyclopenta[b]indoles cytotoxicity in acute myeloid leukemia cells

Firstly, three synthetic cyclopenta[*b*]indoles **1**, **2,** and **3** were tested in ATRA-sensible and ATRA-resistant acute myeloid leukemia cellular models. Among the evaluated compounds, compound **2** presented greater cytotoxic potential for both leukemia cell lines. However, the same cytotoxic potential was not observed for compounds **1** and **3**, which showed less potency and/or efficacy (Fig. 1B). To further characterize the pharmacological proprieties of compound **2**, a dose and time concentration analysis was performed. In both, NB4 and NB4-R2 cells, compound **2** exerts dose- and time-dependent reduction of cell viability at similar extension between ATRA-sensitive and ATRA–resistance cells, as evidenced by the similar IC_{50} (NB4: 1.3 and 1.4 μM; NB4-R2: 1.3 and 1.3 μM, upon 48 and 72 h of exposure, respectively; $P < 0.05$) (Fig. 1C). Colchicine was used as a reference compound in initial assays and its dose and time concentration curves for NB4 and NB4-R2 cells are shown

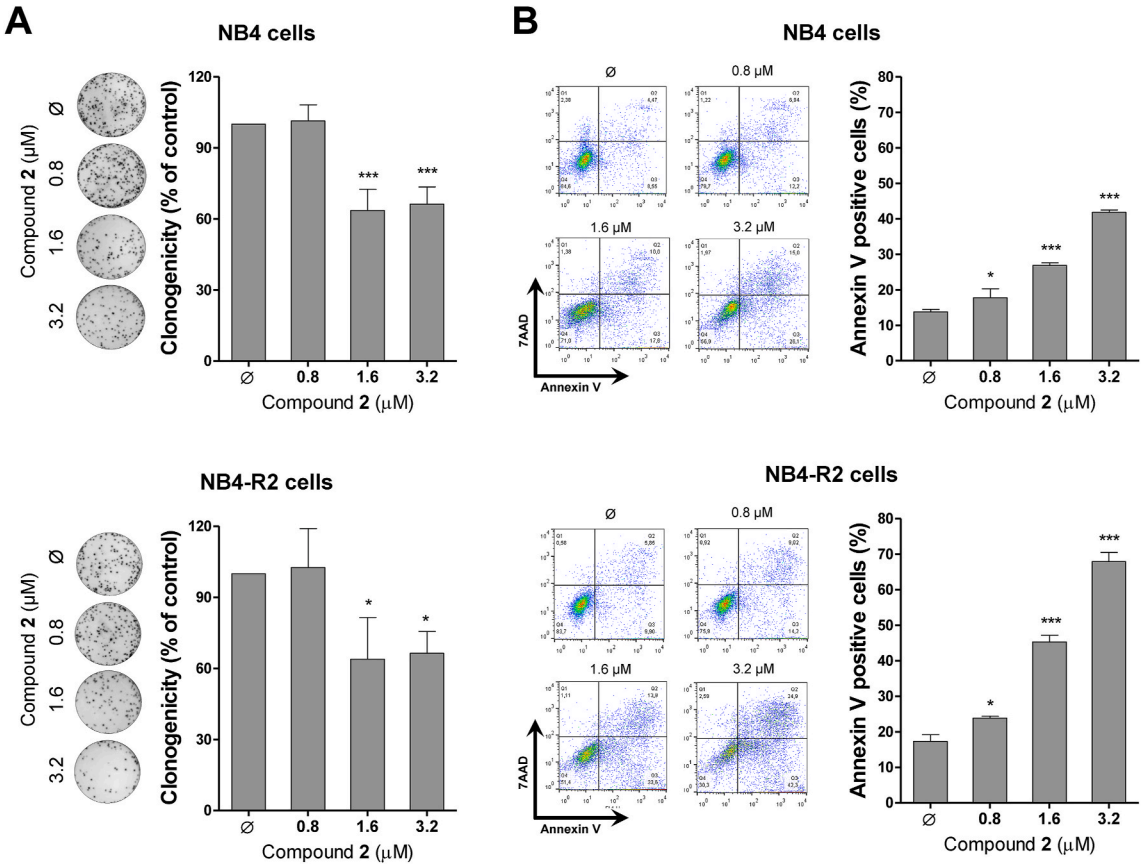

Fig. 2. Compound **2** inhibits autonomous clonal growth and induces apoptosis in NB4 and NB4-R2 cells. **(A)** Colonies containing viable cells were detected by the addition of MTT after 8 days of culture of NB4 and NB4-R2 cells treated with compound **2** (0.8, 1.6, 3.2 μM) for 24 h and normalized to the corresponding DMSO-treated controls (Ø). Colony images are shown for one experiment and the bar graphs show the mean ± S.D. of at least three independent experiments. $^*P < 0.05$; $^{***}P < 0.0001$; ANOVA and Bonferroni post-test. **(B)** Apoptosis was detected by flow cytometry in NB4 and NB4-R2 cells treated with graded concentrations of compound **2** (0.8, 1.6 and 3.6 μM) for 48 h using an annexin V/7AAD staining method. Representative dot plots are shown for each condition; the upper and lower right quadrants (Q2 plus Q3) cumulatively contain the apoptotic population (annexin V+ cells). Bar graphs represent the mean ± S.D. of at least four independent experiments quantifying apoptotic cell death. The *P* values and cell lines are indicated in the graphs; $^*P < 0.05$, $^{**}P < 0.01$; $^{***}P < 0.0001$ for cells treated with compound **2** compared to DMSO-treated (Ø) cells; ANOVA and Bonferroni post-test.

in Supplementary Fig. 1. Of note, compound **2** did not reduce the viability of normal leukocytes, suggesting selectivity for malignant blood cells (IC_{50} > 50 μM; Supplementary Fig. 2).

3.2. Compound **2** decreases autonomous clonal growth and promotes apoptosis and cell cycle arrest in NB4 and NB4-R2 cells

Next, to define the cellular events involved in the reduction of cell viability upon compound **2** treatment, multiple cellular assays were performed. Long-term exposure to compound **2** strongly decreased autonomous clonal growth in both AML cell lines (Fig. 2A). In NB4 and NB4-R2 cells, 48 h of exposure to compound **2** induces significant levels of apoptosis ($P < 0.05$, Fig. 2B).

In the cell cycle analysis, a significant increase in cells in $_{sub}G_1$ was observed in NB4 an NB4-R2 upon compound **2** treatment, which corroborates the findings of apoptosis (all $P < 0.05$, Fig. 3A–B). Additionally, a significant reduction in a concentration-dependent manner of cells at G_0/G_1 was observed ($P < 0.05$), indicating an accumulation of cells in S and G_2/M phases, and failure in the cell cycle progression (Fig. 3C). Due to the large proportion of cells in $_{sub}G_1$ after treatment for 24 h with compound **2** that impacts the distribution of the other cell cycle phases, NB4 and NB4-R2 cells were synchronized with double-thymidine block and the impact of the compound **2** was evaluated during the early progression of the cell cycle. Notably, compound **2** induces a strong cell arrest at G_2/M from 6 h of treatment (Fig. 3D and Supplementary Fig. 3).

3.3. Compound **2** reduces STMN1 expression/activity, and induces apoptosis and DNA damage markers in NB4 and NB4-R2 cells

In the molecular analysis, STMN1 expression and its inactive form (phospho-STMN1^{S16}) (proliferation marker), γH2AX and CHK2 (DNA damage marker) and cleaved PARP1 (apoptosis marker) were investigated by Western blot and a panel of 14 DNA damage-related genes (*BAX, BBC3, CDKN1A, CDKN1B, ERCC1, GADD45A, MSH3, PCNA, PMAIP1, RNF168, RNF8, RPA1, XPC,* and *XRCC3*) were investigated by quantitative RT-PCR. Increased doses of compound **2** significantly reduces STMN1 expression and increases STMN1 phosphorylation, as well, induces H2AX and CHK2 phosphorylation, and PARP1 cleavage in both acute myeloid leukemia cell lines (all $P < 0.05$) (Fig. 4A and B). Among the DNA damage-related genes investigated, 4 out of 14 (*CDKN1A*, *PMAIP1*, *GADD45A*, and *XRCC3*) were significantly modulated by compound **2** in NB4 and NB4-R2 cells (all $P < 0.05$, Fig. 5 and Supplementary Table 2).

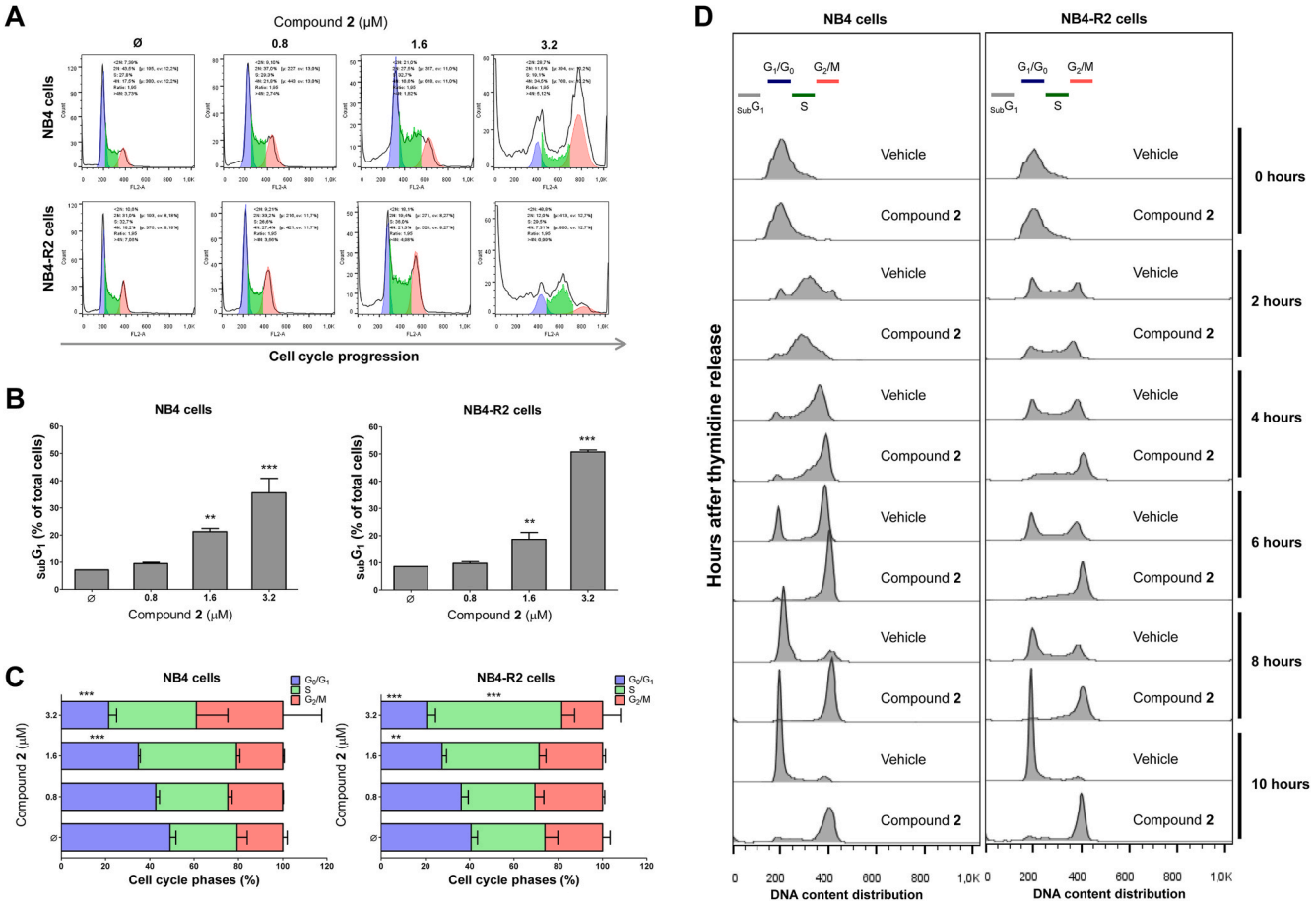

Fig. 3. Compound **2** leads to cell cycle arrest at S and G_2/M phases in acute leukemia cells. **(A)** The phases of the cell cycle were determined by analyzing the DNA content through staining with propidium iodide and flow cytometry in NB4 or NB4-R2 cells treated with compound **2** (0.8, 1.6 or 3.2 μM) or vehicle for 48 h. A representative histogram for each condition is illustrated. **(B)** The bar graph represents the mean ± S.D. of the percentages of cells in $_{sub}G_1$ from at least three independent experiments. **(C)** The mean ± S.D. of the cell distributions that are in the G_0/G_1, S and G_2/M phases of the cell cycle (excluding $_{sub}G_1$) of at least three independent experiments are represented in the bar graph. The values of *P* and cell lines are indicated in the graphs; *$P < 0.05$, **$P < 0.01$, ***$P < 0.001$ for DMSO-treated (Ø) cells *vs.* compound **2**; ANOVA and Bonferroni post-test. **(D)** NB4 and NB4-R2 cells were synchronized by a double-thymidine block. After thymidine release, cells were treated with vehicle or compound **2** (3.2 μM), collected every 2 h (five time points) and DNA content distribution was evaluated by FACS as indicated.

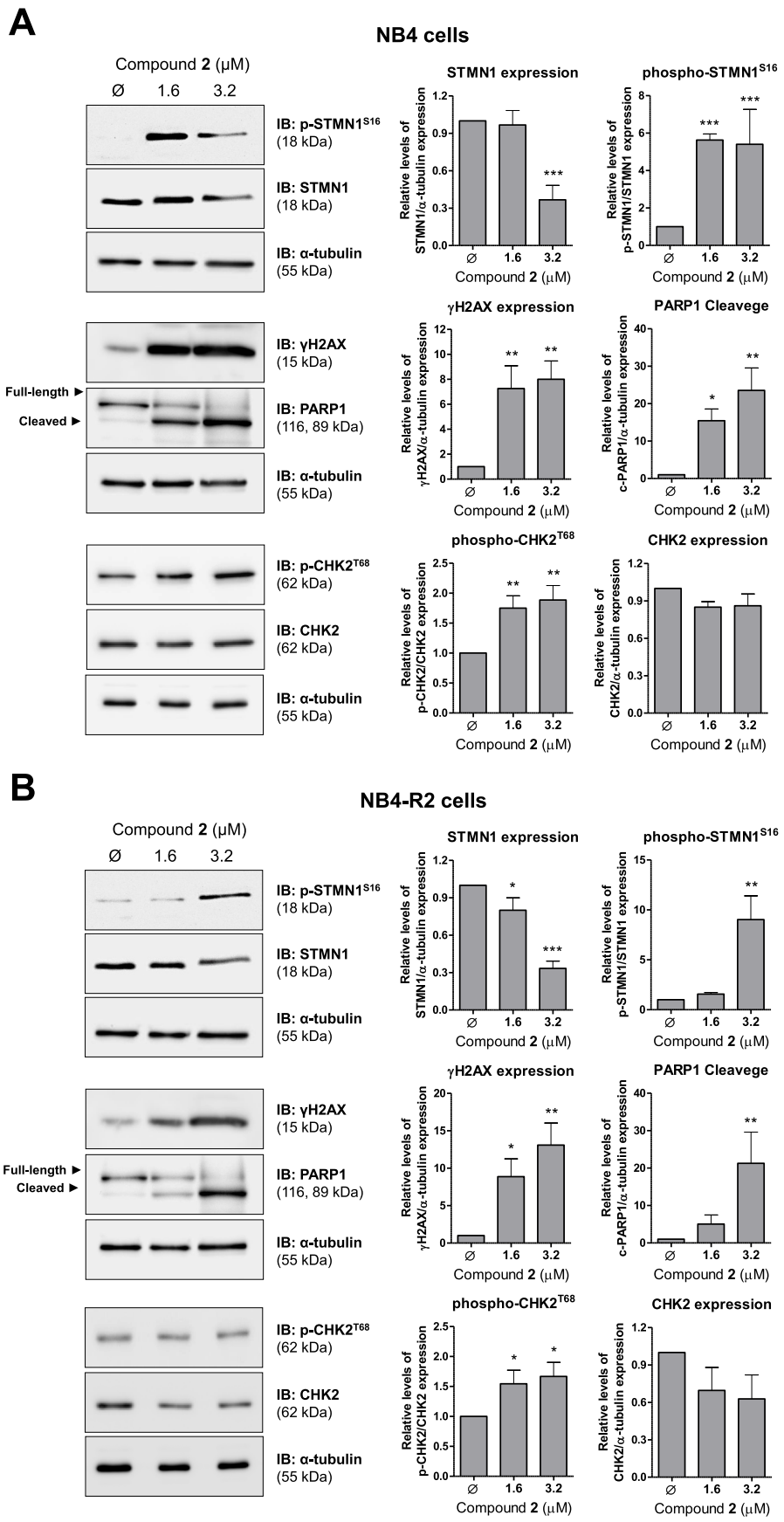

Fig. 4. Compound **2** induces molecular markers of DNA damage and apoptosis in NB4 and NB4-R2 cells. **(A)** Western blot analysis for levels of phospho (p)-Stathmin 1^{S16}, STMN1, γH2AX, p-$CHK2^{T68}$, CHK2, and PARP1 (total and cleaved) in total cell extracts of NB4 and NB4-R2 cells treated with compound **2** (0.8, 1.6 or 3.2 μM) or vehicle for 48 h; The membranes were incubated with the indicated antibodies and developed with the SuperSignal ™ West Dura Extended Duration Substrate and Gel Doc XR + system. **(B)** Bar graphs represent the mean ± S.D. of three independent experiments quantifying band intensities of indicated proteins. $^{*}P < 0.05$, $^{**}P < 0.01$, $^{***}P < 0.001$; ANOVA and Bonferroni post-test. Note that compound **2** treatment induces Stathmin 1 phosphorylation at serine 16 site (an inhibitory site), H2AX phosphorylation at serine 139 and CHK2 at threonine 68 (DNA damage markers) and PARP1 cleavage (an apoptosis marker) in NB4 and NB4-R2 cells.

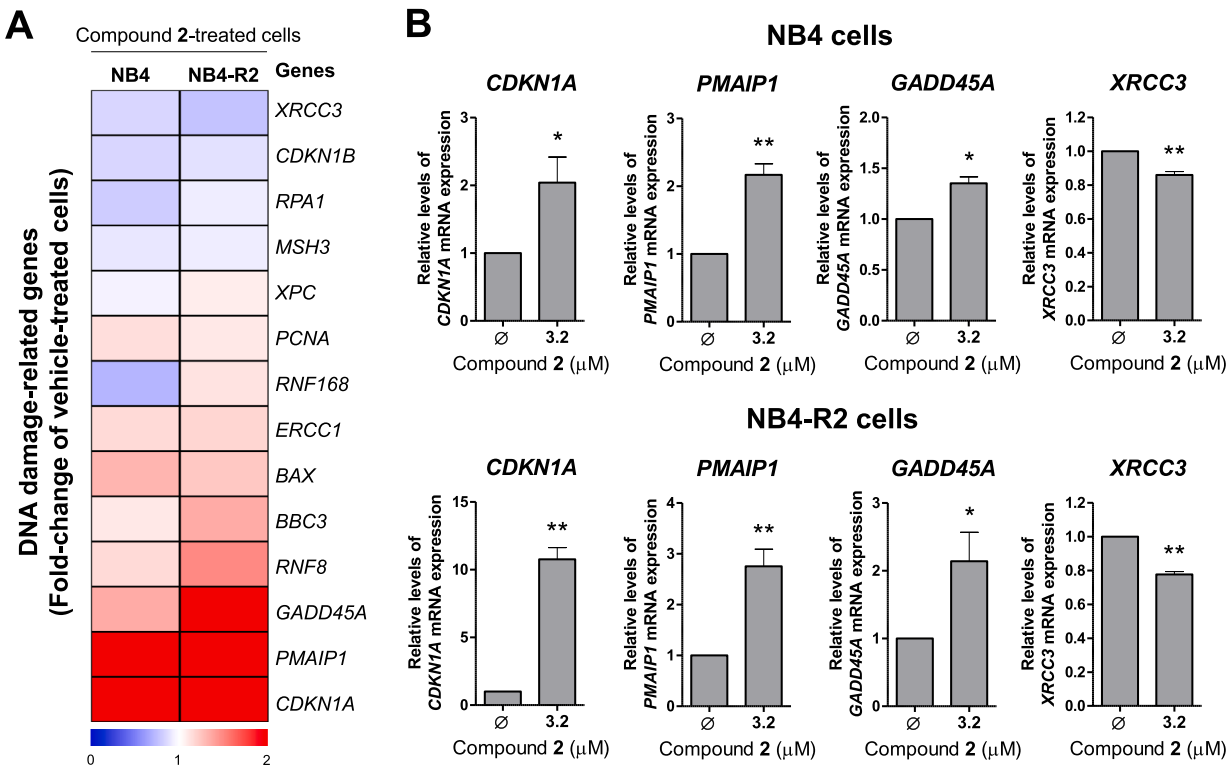

Fig. 5. Compound **2** modulates *CDKN1A*, *PMAIP1*, *GADD45A*, and *XRCC3* in NB4 and NB4-R2 cells. (**A**) The heatmap illustrates the quantitative RT-PCR analysis of the DNA damage-related genes in NB4 and NB4-R2 cells upon treatment with compound **2** (3.2 μM; mean; n = 3) for 48 h. The data are represented as fold-change of vehicle-treated cells, down and upregulated genes are given by blue and red, respectively. **(B)** The bar graph represents mean ± S.D. of the fold-change of vehicle-treated cells for *CDKN1A*, *PMAIP1*, *GADD45A*, and *XRCC3* in NB4 and NB4-R2 cells upon compound **2** (3.2 μM; mean; n = 3) exposure for 48 h. The *p* values and cell lines are indicated in the graphs; $^{*}P < 0.05$; $^{**}P < 0.01$; Student *t* test.

*3.4. Compound **2** causes microtubule instability and generates mitotic aberrations in NB4 and NB4-R2 cells*

NB4 and NB4-R2 cells stained with H&E and analyzed by optical microscopy showed a high frequency of mitotic aberrations after treatment with 1.6 μM of compound **2** for 48 h (Fig. 6A). Since compound **2** induces a strong G_2/M arrest after 6 h of thymidine release in synchronized NB4 and NB4-R2 cells, we evaluated nuclear and microtubules morphology through immunofluorescence at this time point. In NB4 and NB4-R2 cells, compound **2** induced diffuse tubulin staining, indicating instability of microtubules, also, cells with condensed chromosomes or large nuclei were observed, indicating failure to complete mitosis, which corroborates the data obtained in flow cytometry (Fig. 6B). Quantitative data analysis confirms that 6 h after the thymidine block release, vehicle-treated cells present a higher proportion in interphase (G_0/G_1), which indicates the ability of these cells to complete the mitosis. In contrast, the proportion of compound **2**-treated NB4 and NB4-R2 cells with large nuclei or aberrant mitotic spindle were significantly increased ($P < 0.05$; Fig. 6B). Moreover, *in vivo* tubulin assay indicates that compound **2** leads to reduction of microtubule polymerization (Fig. 6C). In docking analysis, two main interactions for compound **2** and tubulin colchicine site were observed: one with the sp^2 oxygen atom of the carboxyl group and other with a sp^3 oxygen atom of the dioxolane five-membered ring, indicating that compound **2** has more efficient interactions than compounds **1** and **3** at the tubulin colchicine site (Fig. 6D).

4. Discussion

Herein, the anti-leukemia effects of novel synthetic cyclopenta[*b*]indoles in ATRA-sensitive and -resistant APL cell lines were investigated. Cyclopenta[*b*]indoles are present in several biologically active natural and synthetic compounds, being directly responsible for their biological effects (Baran and Richter, 2005; Richter et al., 2008; Uhlig et al., 2009). Among biological functions described for compounds that contain the cyclopenta[*b*]indole portion have been reported abortive and anti-estrogenic activities, prostaglandin D2 receptor antagonist activity, progesterone receptor agonist activity, antioxidant and insecticidal activity (Levesque et al., 2007; Nicoll-Griffith et al., 2007; Qiao et al., 2010; Ratni et al., 2009; Roll et al., 2009; Sturino et al., 2007; Talaz et al., 2009; Wong et al., 1998).

Due to the great relevance of these class of compound, several synthetic protocols have been described to synthesize this heterocyclic nucleus, such as Fischer indolization, Friedel-Crafts intramolecular reaction and palladium-catalyzed cyclization, but many of these protocols have low yield and low stereoselectivity (Sorensen and Pombo-Villar, 2004; Xu et al., 2012). The cyclopenta[*b*]indoles used for the present study were obtained using a sequence of reactions using Morita-Baylis-Hillman (MBH) adducts as building blocks and Indium Chloride III as an acid catalyst (Supplementary Information). The differential of this synthesis is that it is a diastereoselective synthesis, already reported by our research group (Santos et al., 2016), which also evaluated the effects of some cyclopenta[*b*]indoles against a panel of human tumor cell lines. Some of the tested cyclopenta[*b*]indoles showed antitumor activity like doxorubicin, but with better selectivity. For instance, the cyclopenta[*b*]indole derivative substituted by a 4-methoxyphenyl group at C3 (methyl-7-hydroxy-3-(4-methoxyphenyl)-1,2,3,4-tetrahydrocyclopenta[*b*]indole-2-carboxylate) presented 12 times more potency than doxorubicin to completely inhibit the cell growth in ovarian cancer cell lines, OVCAR-3 (Santos et al., 2016).

In the present study, among the three pure enantiomer of novel synthetic cyclopenta[*b*]indoles tested, compound **2** displayed higher

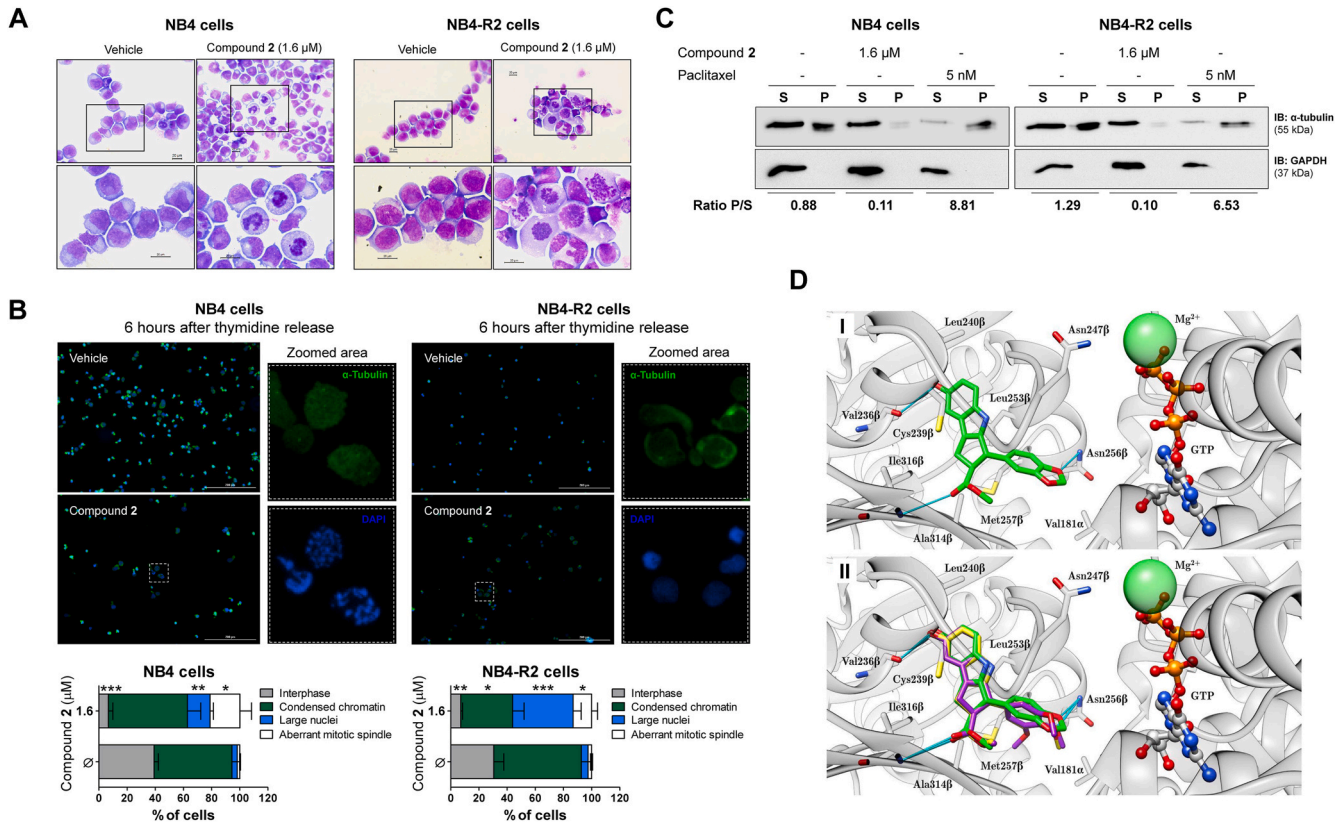

Fig. 6. Compound **2** treatment generates aberrant mitoses and microtubule instability in leukemia cell lines. **(A)** NB4 and NB4-R2 cells were treated with vehicle or compound **2** (1.6 μM) for 48 h, fixed and stained with hematoxylin and eosin (H&E). 400 × and 1000 × magnification images are illustrated. **(B)** Nuclear and microtubules morphology was evaluated by immunofluorescence analysis in synchronized NB4 and NB4-R2 cells treated with vehicle or compound **2** after 6 h of thymidine release. The zoomed area displays details in compound **2**-treated NB4 or NB4-R2, α-Tubulin (green) and DAPI (blue). Scale bars are shown in figure (200 μm). Bar graphs represent the mean ± S.D. of the proportion of NB4 or NB4-R2 treated with vehicle or compound **2** from three independent experiments (at least 150 cells per condition), which were classified according to morphology into interphase, cells with a condensed nucleus (mitosis), large nuclei or aberrant mitotic spindle. $^{*}P < 0.05$, $^{**}P < 0.01$, $^{***}P < 0.001$; Student *t* test. **(C)** NB4 and NB4-R2 cells were treated with vehicle or compound **2** (1.6 μM) for 48 h and submitted extraction of the soluble (S) and precipitated (P) cellular fractions and Western blot. Free tubulin is present in fraction S, while polymerized tubulin is present in fraction P. The expression of GAPDH, which is present only in fraction S, was used to verify the efficiency of fractionation. Paclitaxel was used as a control for the polymerization of microtubules. The ratio of α-tubulin present in fractions S and P are described. The membranes were incubated with the indicated antibodies and developed with the SuperSignal ™ West Dura Extended Duration Substrate and Gel Doc XR + system. **(D)** Conformation proposal of the interaction compound **2** (panel I) on the binding site of colchicine of the tubulin compared with the interactions of compounds **1** and **3** (panel II).

cytotoxic effects, reduced autonomous clonal growth, which is usually associated with aggressiveness in leukemia (Lowenberg et al., 1993), and induced apoptosis and cell cycle arrest in ATRA sensible and resistant APL cells. Additionally, compound **2** did not exhibit cytotoxicity in normal leukocytes, which suggest selectivity for malignant hematopoietic cells. Of note, initial observations using NB4 as a cellular model of APL generate evidence of the therapeutic potential of ATRA and arsenic trioxide (Idres et al., 2001; Shao et al., 1998), which are currently the first line of treatment in this disease with clinical outcomes superior to previous therapeutic options (Rego et al., 2013). NB4-R2 is a ATRA-resistant subclone of the NB4 APL cell line, which changes the amino acid Gln903 to an in-phase stop codon, generating a truncated form of PML-RARα which has lost 52 amino acids at its C-terminal (Duprez et al., 2000). In the clinic, ATRA resistance represents a therapeutic challenge in the treatment of APL and new therapeutic options are of interest (Baljevic et al., 2011; Noguera et al., 2019).

In the molecular scenario, compound **2** reduced STMN1 expression, and induced PARP1 cleavage, H2AX and CHK2 phosphorylation. In acute leukemia cells, STMN1 plays an important role in cell cycle progression and clonogenicity, being a proliferation marker of normal and malignant hematopoietic cells (Machado-Neto et al., 2014a, 2014b). In malignant tumors, STMN1 integrates multiple signaling pathways by regulation of microtubule dynamics, sequestering free tubulin dimers or directly inducing microtubule-catastrophe, and high STMN1 expression has been associated with acceleration in mitosis, migration, and invasion (Belletti and Baldassarre, 2011). Despite the importance of STMN1 in the malignant type of several types of hematological and solid cancers, effective pharmacological inhibitors of STMN1 have not yet been described (Biaoxue et al., 2016). PARP1 is one of several known cellular substrates of caspases and be cleaved and inactivated by active caspases 3 and 7 and this cleavage is considered as a hallmark of apoptosis forming fragments of 24 kDa and 89 kDa (Castri et al., 2014; Desroches and Denault, 2019).

H2AX is a variant of the H2A protein family, which is a component of the histone octamer in nucleosomes. In the presence of DNA damage, H2AX is phosphorylated at the serine 139, being called γH2AX (Kuo and Yang, 2008; Rogakou et al., 1998, 1999). Similarly, CHK2 is also phosphorylated upon DNA damage (Zannini et al., 2014). In the *in vivo* tubulin polymerization assay, NB4 and NB4-R2 cells showed a great reduction in the levels of polymerized tubulin. The accumulation of DNA damage is one of the hallmarks of the mitotic catastrophe, a type of cell death that occurs during mitosis (Castedo et al., 2004). Among the DNA damage-related genes investigated, *CDKN1A*, *GADD45A*, *PMAIP1*, and *XRCC3* were modulated by compound **2** in NB4 and NB4-R2 cells. CDKN1A and GADD45A expressions are induced by DNA damage and associated with growth arrest and apoptosis (Kreis et al., 2019; Salvador

et al., 2013). PMAIP1 (also known as NOXA) is a BH3-only member of the BCL2 family that acts as a pro-apoptotic protein, and its expression is also activated in response to DNA damage (Morsi et al., 2018). XRCC3 plays a role in DNA double-strand break/recombinational repair to maintain chromosome stability, and its downregulation have been associated with increased chemotherapy-induced apoptosis (Roos et al., 2018). Taken together, these data indicated that the compound **2** disturbs microtubule dynamics, which reduces cell viability by cell cycle arrest and DNA damage, ultimately, triggering apoptosis.

Regarding structure-activity, our results suggest that the trimethoxy that has the freest O-methyl groups presented the lower cytotoxic activity, and when their freedom were restricted using the O-CH_2-CH_2-O, the cytotoxic activity increased, being even improved by restricting it even more with O-CH_2-O. These data suggest that the restriction of the freedom groups favors interactions of hydrogen bonding with functional groups in the active site. Molecular *docking* experiments support this hypothesis, since the main interactions, one with the sp^2 oxygen atom of the carboxyl group and other with a sp^3 oxygen atom of the dioxolane five-membered ring, were observed for compound **2**.

In summary, the present study identified a novel synthetic cyclopenta[*b*]indole that display antineoplastic effects, inducing cell cycle deregulation and apoptosis in NB4 and NB4-R2 cell lines. Our exploratory molecular analysis identified reduction of proliferation markers and tubulin stability, and induction of DNA damage and apoptosis markers. These results shed light on the structure-activity relationship of cyclopenta[*b*]indoles allowing new molecular modifications to improve potency and selectivity, increasing the antineoplastic arsenal.

CRediT authorship contribution statement

Hugo Passos Vicari: Data curation, Formal analysis, Investigation, Methodology, Writing - original draft. **Keli Lima:** Investigation, Methodology, Writing - review & editing. **Ralph da Costa Gomes:** Investigation, Methodology, Writing - review & editing. **Daniara Cristina Fernandes:** Investigation, Methodology, Writing - review & editing. **Jean Carlos Lipreri da Silva:** Investigation, Methodology, Writing - review & editing. **Manoel Trindade Rodrigues Junior:** Investigation, Methodology, Writing - review & editing. **Aline Silva Barroso de Oliveira:** Investigation, Methodology, Writing - review & editing. **Ricardo Nascimento dos Santos:** Investigation, Methodology, Writing - review & editing. **Adriano Defini Andricopulo:** Funding acquisition, Investigation, Writing - review & editing. **Fernando Coelho:** Conceptualization, Formal analysis, Funding acquisition, Supervision, Writing - original draft. **Leticia Veras Costa-Lotufo:** Conceptualization, Formal analysis, Funding acquisition, Supervision, Writing - original draft. **João Agostinho Machado-Neto:** Conceptualization, Data curation, Funding acquisition, Project administration, Supervision, Writing - original draft.

Declaration of competing interest

The authors declare no conflict of interest.

Acknowledgments

This study was supported by the grant #2017/24993-0, #2019/23864-7 #2019/01700-2, and #2015/17177-6, São Paulo Research Foundation (FAPESP), and grant #402587/2016-2, Conselho Nacional de Desenvolvimento Científico e Tecnológico (CNPq), and Coordenação de Aperfeiçoamento de Pessoal de Nível Superior (CAPES). F.C. and A.D.A. thank also FAPESP for financial support (#2013/07600-3). F.C. thanks also to CNPq for grants #422890/2016-2 and #301330/2018-2.

Appendix A. Supplementary data

Supplementary data to this article can be found online at https://doi.org/10.1016/j.ejphar.2021.173853.

References

Arber, D.A., Orazi, A., Hasserjian, R., Thiele, J., Borowitz, M.J., Le Beau, M.M., Bloomfield, C.D., Cazzola, M., Vardiman, J.W., 2016. The 2016 revision to the World Health Organization classification of myeloid neoplasms and acute leukemia. Blood 127, 2391–2405.

Avvisati, G., Lo Coco, F., Mandelli, F., 2001. Acute promyelocytic leukemia: clinical and morphologic features and prognostic factors. Semin. Hematol. 38, 4–12.

Baljevic, M., Park, J.H., Stein, E., Douer, D., Altman, J.K., Tallman, M.S., 2011. Curing all patients with acute promyelocytic leukemia: are we there yet? Hematol. Oncol. Clin. N. Am. 25, 1215–1233 viii.

Baran, P.S., Richter, J.M., 2005. Enantioselective total syntheses of welwitindolinone A and fischerindoles I and G. J. Am. Chem. Soc. 127, 15394–15396.

Belletti, B., Baldassarre, G., 2011. Stathmin: a protein with many tasks. New biomarker and potential target in cancer. Expert Opin. Ther. Targets 15, 1249–1266.

Bennett, J.M., Catovsky, D., Daniel, M.T., Flandrin, G., Galton, D.A., Gralnick, H.R., Sultan, C., 1976. Proposals for the classification of the acute leukaemias. French-American-British (FAB) co-operative group. Br. J. Haematol. 33, 451–458.

Biaoxue, R., Xiguang, C., Hua, L., Shuanying, Y., 2016. Stathmin-dependent molecular targeting therapy for malignant tumor: the latest 5 years' discoveries and developments. J. Transl. Med. 14, 279.

Castedo, M., Perfettini, J.L., Roumier, T., Andreau, K., Medema, R., Kroemer, G., 2004. Cell death by mitotic catastrophe: a molecular definition. Oncogene 23, 2825–2837.

Castri, P., Lee, Y.J., Ponzio, T., Maric, D., Spatz, M., Bembry, J., Hallenbeck, J., 2014. Poly(ADP-ribose) polymerase-1 and its cleavage products differentially modulate cellular protection through NF-kappaB-dependent signaling. Biochim. Biophys. Acta 1843, 640–651.

De Kouchkovsky, I., Abdul-Hay, M., 2016. 'Acute myeloid leukemia: a comprehensive review and 2016 update. Blood Canc. J. 6, e441.

Desroches, A., Denault, J.B., 2019. Caspase-7 uses RNA to enhance proteolysis of poly (ADP-ribose) polymerase 1 and other RNA-binding proteins. Proc. Natl. Acad. Sci. U. S. A. 116, 21521–21528.

Duprez, E., Benoit, G., Flexor, M., Lillehaug, J.R., Lanotte, M., 2000. A mutated PML/RARA found in the retinoid maturation resistant NB4 subclone, NB4-R2, blocks RARA and wild-type PML/RARA transcriptional activities. Leukemia 14, 255–261.

Duprez, E., Ruchaud, S., Houge, G., Martin-Thouvenin, V., Valensi, F., Kastner, P., Berger, R., Lanotte, M., 1992. A retinoid acid 'resistant' t(15;17) acute promyelocytic leukemia cell line: isolation, morphological, immunological, and molecular features. Leukemia 6, 1281–1287.

Idres, N., Benoit, G., Flexor, M.A., Lanotte, M., Chabot, G.G., 2001. Granulocytic differentiation of human NB4 promyelocytic leukemia cells induced by all-trans retinoic acid metabolites. Canc. Res. 61, 700–705.

Kitamura, K., Kiyoi, H., Yoshida, H., Saito, H., Ohno, R., Naoe, T., 1997. Mutant AF-2 domain of PML-RARalpha in retinoic acid-resistant NB4 cells: differentiation induced by RA is triggered directly through PML-RARalpha and its down-regulation in acute promyelocytic leukemia. Leukemia 11, 1950–1956.

Kreis, N.N., Louwen, F., Yuan, J., 2019. The multifaceted p21 (Cip1/Waf1/CDKN1A) in cell differentiation, migration and cancer therapy. Cancers (Basel) 11.

Kuo, L.J., Yang, L.X., 2008. Gamma-H2AX - a novel biomarker for DNA double-strand breaks. In Vivo 22, 305–309.

Levesque, J.F., Day, S.H., Chauret, N., Seto, C., Trimble, L., Bateman, K.P., Silva, J.M., Berthelette, C., Lachance, N., Boyd, M., et al., 2007. Metabolic activation of indole-containing prostaglandin D2 receptor 1 antagonists: impacts of glutathione trapping and glucuronide conjugation on covalent binding. Bioorg. Med. Chem. Lett 17, 3038–3043.

Livak, K.J., Schmittgen, T.D., 2001. Analysis of relative gene expression data using real-time quantitative PCR and the 2(-Delta Delta C(T)) Method. Methods 25, 402–408.

Lowenberg, B., van Putten, W.L., Touw, I.P., Delwel, R., Santini, V., 1993. Autonomous proliferation of leukemic cells in vitro as a determinant of prognosis in adult acute myeloid leukemia. N. Engl. J. Med. 328, 614–619.

Machado-Neto, J.A., de Melo Campos, P., Favaro, P., Lazarini, M., Lorand-Metze, I., Costa, F.F., Olalla Saad, S.T., Traina, F., 2014a. Stathmin 1 is involved in the highly proliferative phenotype of high-risk myelodysplastic syndromes and acute leukemia cells. Leuk. Res. 38, 251–257.

Machado-Neto, J.A., Saad, S.T., Traina, F., 2014b. Stathmin 1 in normal and malignant hematopoiesis. BMB Rep. 47, 660–665.

Melnick, A., Licht, J.D., 1999. Deconstructing a disease: RARalpha, its fusion partners, and their roles in the pathogenesis of acute promyelocytic leukemia. Blood 93, 3167–3215.

Mistry, S.J., Atweh, G.F., 2001. Stathmin inhibition enhances okadaic acid-induced mitotic arrest: a potential role for stathmin in mitotic exit. J. Biol. Chem. 276, 31209–31215.

Morsi, R.Z., Hage-Sleiman, R., Kobeissy, H., Dbaibo, G., 2018. Noxa: role in cancer pathogenesis and treatment. Curr. Cancer Drug Targets 18, 914–928.

Nason-Burchenal, K., Maerz, W., Albanell, J., Allopenna, J., Martin, P., Moore, M.A., Dmitrovsky, E., 1997. Common defects of different retinoic acid resistant promyelocytic leukemia cells are persistent telomerase activity and nuclear body disorganization. Differentiation 61, 321–331.

Nicoll-Griffith, D.A., Seto, C., Aubin, Y., Levesque, J.F., Chauret, N., Day, S., Silva, J.M., Trimble, L.A., Truchon, J.F., Berthelette, C., et al., 2007. In vitro biotransformations of the prostaglandin D2 (DP) antagonist MK-0524 and synthesis of metabolites. Bioorg. Med. Chem. Lett 17, 301–304.

Noguera, N.I., Catalano, G., Banella, C., Divona, M., Faraoni, I., Ottone, T., Arcese, W., Voso, M.T., 2019. Acute promyelocytic leukemia: update on the mechanisms of leukemogenesis, resistance and on innovative treatment strategies. Cancers (Basel) 11.

Qiao, M.F., Ji, N.Y., Liu, X.H., Li, K., Zhu, Q.M., Xue, Q.Z., 2010. Indoloditerpenes from an algicolous isolate of Aspergillus oryzae. Bioorg. Med. Chem. Lett 20, 5677–5680.
Ratni, H., Blum-Kaelin, D., Dehmlow, H., Hartman, P., Jablonski, P., Masciadri, R., Maugeais, C., Patiny-Adam, A., Panday, N., Wright, M., 2009. Discovery of tetrahydro-cyclopenta[b]indole as selective LXRs modulator. Bioorg. Med. Chem. Lett 19, 1654–1657.
Rego, E.M., Kim, H.T., Ruiz-Arguelles, G.J., Undurraga, M.S., Uriarte Mdel, R., Jacomo, R.H., Gutierrez-Aguirre, H., Melo, R.A., Bittencourt, R., Pasquini, R., et al., 2013. Improving acute promyelocytic leukemia (APL) outcome in developing countries through networking, results of the International Consortium on. APL. Blood 121, 1935–1943.
Reiter, A., Lengfelder, E., Grimwade, D., 2004. Pathogenesis, diagnosis and monitoring of residual disease in acute promyelocytic leukaemia. Acta Haematol. 112, 55–67.
Richter, J.M., Ishihara, Y., Masuda, T., Whitefield, B.W., Llamas, T., Pohjakallio, A., Baran, P.S., 2008. Enantiospecific total synthesis of the hapalindoles, fischerindoles, and welwitindolinones via a redox economic approach. J. Am. Chem. Soc. 130, 17938–17954.
Rogakou, E.P., Boon, C., Redon, C., Bonner, W.M., 1999. Megabase chromatin domains involved in DNA double-strand breaks in vivo. J. Cell Biol. 146, 905–916.
Rogakou, E.P., Pilch, D.R., Orr, A.H., Ivanova, V.S., Bonner, W.M., 1998. DNA double-stranded breaks induce histone H2AX phosphorylation on serine 139. J. Biol. Chem. 273, 5858–5868.
Roll, D.M., Barbieri, L.R., Bigelis, R., McDonald, L.A., Arias, D.A., Chang, L.P., Singh, M. P., Luckman, S.W., Berrodin, T.J., Yudt, M.R., 2009. The lecanindoles, nonsteroidal progestins from the terrestrial fungus Verticillium lecanii 6144. J. Nat. Prod. 72, 1944–1948.
Roos, W.P., Frohnapfel, L., Quiros, S., Ringel, F., Kaina, B., 2018. XRCC3 contributes to temozolomide resistance of glioblastoma cells by promoting DNA double-strand break repair. Canc. Lett. 424, 119–126.
Rowley, J.D., Golomb, H.M., Vardiman, J., Fukuhara, S., Dougherty, C., Potter, D., 1977. Further evidence for a non-random chromosomal abnormality in acute promyelocytic leukemia. Int. J. Canc. 20, 869–872.
Salvador, J.M., Brown-Clay, J.D., Fornace Jr., A.J., 2013. Gadd45 in stress signaling, cell cycle control, and apoptosis. Adv. Exp. Med. Biol. 793, 1–19.
Santos, M.S., Fernandes, D.C., Rodrigues Jr., M.T., Regiani, T., Andricopulo, A.D., Ruiz, A.L., Vendramini-Costa, D.B., de Carvalho, J.E., Eberlin, M.N., Coelho, F., 2016. Diastereoselective synthesis of biologically active cyclopenta[b]indoles. J. Org. Chem. 81, 6626–6639.
Sanz, M.A., Grimwade, D., Tallman, M.S., Lowenberg, B., Fenaux, P., Estey, E.H., Naoe, T., Lengfelder, E., Buchner, T., Dohner, H., et al., 2009. Management of acute promyelocytic leukemia: recommendations from an expert panel on behalf of the European LeukemiaNet. Blood 113, 1875–1891.
Shao, W., Fanelli, M., Ferrara, F.F., Riccioni, R., Rosenauer, A., Davison, K., Lamph, W. W., Waxman, S., Pelicci, P.G., Lo Coco, F., et al., 1998. Arsenic trioxide as an inducer of apoptosis and loss of PML/RAR alpha protein in acute promyelocytic leukemia cells. J. Natl. Cancer Inst. 90, 124–133.
Short, N.J., Rytting, M.E., Cortes, J.E., 2018. Acute myeloid leukaemia. Lancet 392, 593–606.
Sorensen, U.S., Pombo-Villar, E., 2004. Synthesis of cyclopenta[b]indol-1-ones and carbazol-4-ones fromN-(2-Halophenyl)-substituted enaminones by intramolecular heck reaction. Helv. Chim. Acta 87, 82–89.
Sturino, C.F., O'Neill, G., Lachance, N., Boyd, M., Berthelette, C., Labelle, M., Li, L., Roy, B., Scheigetz, J., Tsou, N., et al., 2007. Discovery of a potent and selective prostaglandin D2 receptor antagonist, [(3R)-4-(4-chloro-benzyl)-7-fluoro-5-(methylsulfonyl)-1,2,3,4-tetrahydrocyclopent a[b]indol-3-yl]-acetic acid (MK-0524). J. Med. Chem. 50, 794–806.
Talaz, O., Gulcin, I., Goksu, S., Saracoglu, N., 2009. Antioxidant activity of 5,10-dihydroindeno[1,2-b]indoles containing substituents on dihydroindeno part. Bioorg. Med. Chem. 17, 6583–6589.
Uhlig, S., Botha, C.J., Vralstad, T., Rolen, E., Miles, C.O., 2009. Indole-diterpenes and ergot alkaloids in Cynodon dactylon (Bermuda grass) infected with Claviceps cynodontis from an outbreak of tremors in cattle. J. Agric. Food Chem. 57, 11112–11119.
Van den Berghe, H., 1988. Morphologic, immunologic and cytogenetic (MIC) working classification of the acute myeloid leukaemias. Second MIC Cooperative Study Group. Br. J. Haematol. 68, 487–494.
Wang, Z.Y., Chen, Z., 2008. Acute promyelocytic leukemia: from highly fatal to highly curable. Blood 111, 2505–2515.
Wong, D.C., Fong, W.P., Lee, S.S., Kong, Y.C., Cheng, K.F., Stone, G., 1998. Induction of estradiol-2-hydroxylase and ethoxyresorufin-O-deethylase by 3-substituted indole compounds. Eur. J. Pharmacol. 362, 87–93.
Xu, B., Guo, Z.L., Jin, W.Y., Wang, Z.P., Peng, Y.G., Guo, Q.X., 2012. Multistep one-pot synthesis of enantioenriched polysubstituted cyclopenta[b]indoles. Angew Chem. Int. Ed. Engl. 51, 1059–1062.
Zannini, L., Delia, D., Buscemi, G., 2014. CHK2 kinase in the DNA damage response and beyond. J. Mol. Cell Biol. 6, 442–457.